Journal of Alloys and Compounds, 190 (1993) 287–290
JALCOM 475

EPR spectra of nanocrystalline composite oxides $La_{1-x}Sr_xFeO_3$ with a perovskite structure

Xi Li, Hengbin Zhang, Shujia Li, Yaoquan Xin and Muyu Zhao
Department of Chemistry, Jilin University, Changchun, 130023 (People's Republic of China)

(Received March 26, 1992; in final form August 8, 1992)

Abstract

Nanocrystals $La_{1-x}Sr_xFeO_3$ ($x=0.0$, 0.1, 0.2, 0.4 and 0.6), containing crystal grains of mean diameter 12.4 nm ($x=0.0$) and 4–7 nm ($x=0.1$–0.6), were compacted into nanocrystalline solid materials under static pressures of 0.5, 1.0 and 1.5 GPa in the axial direction at ambient temperature. The results showed that the peak intensities of the electron paramagnetic resonance (EPR) spectra for the nanocrystalline solid materials were about 10^3–10^4 times stronger than those of conventional crystals. The EPR spectra changed with grain size and compacting pressure. The characteristics of the EPR spectra of these nanocrystalline solid materials are discussed.

1. Introduction

Nanocrystalline solids are a new type of polycrystalline material. The sizes of the crystalline grains are in the range 1–10 nm [1], 5–15 nm [2] or 2–20 nm [3]. With regard to the structure, the materials possess two different regions: lattice and surface [1]; atoms in the lattice lie in an ordered environment, whereas those at the surface lie in the interfacial region with a strongly distorted structure. The chemical bonds between the atoms may be covalent or ionic. Interfacial atoms in the "naked state" are very different from the atoms in the bulk phase with respect to their coordinate status.

Composite oxides differ from simple metals or oxides. The distribution and change of the various components in the composite oxide are complex because of the variety of components and the random orientation of the crystallites.

Nanocrystalline solid materials have received considerable attention from materials scientists. The optical, electrical and mechanical properties of nanocrystalline materials have been studied [4–6]. Electron paramagnetic resonance (EPR) spectra have been used to characterize the nanocrystalline metal Er [7]. However, nanocrystalline composite oxides have not been studied in detail, although conventional polycrystalline materials have been extensively used. In order to understand the relationship between structure and properties, it is necessary to examine the bonding state of interfacial atoms and the difference between nanocrystalline composite oxides and simple metals, as well as conventional composite oxides.

2. Experimental details

$La_{1-x}Sr_xFeO_3$ samples A ($x=0.0$), B ($x=0.1$), C ($x=0.2$) and D ($x=0.4$) were prepared by the polyethylene glycol method [8]. The mean diameters of the crystalline grains were 12.6 nm (A), 6 nm (B), 4 nm (C) and 7 nm (D). Sample E (8 nm, $x=0.6$) was prepared by the polyvinyl alcohol method [9]. The samples A–E were obtained after calcining the precursors at 400–550 °C for 2 h. X-Ray diffraction (XRD) analysis showed that samples A, B, C and D consist of single orthorhombic phase, but the $2La_2O_3 \cdot SrO$ mixed phase was present in sample E. Samples F ($x=0.1$), G ($x=0.2$) and H ($x=0.4$) with conventional crystals were obtained after calcining the precursors (prepared by the polyethylene glycol method) at 1000 °C for 8 h. The mean diameters of the crystalline grains for samples F, G and H were 82, 60 and 70 nm respectively. The nanocrystalline powders were compacted into pellets with a diameter of 11.28 mm and a thickness of 0.04–0.07 mm under axial pressures of 0.5, 1.0 and 1.5 GPa at ambient temperature. The pellets were then broken into several pieces for EPR measurement.

The EPR spectra of the samples (A–H) were recorded using a Brucker ER 200D EPR spectrometer at ambient temperature. The relative intensity (RI) of the EPR spectra was measured by double integral calculus and transformed into the relative intensity per milligram of sample (RI mg^{-1}).

0925-8388/93/$6.00

3. Results and discussion

3.1. Structural features of nanocrystalline materials

In the nanocrystalline composite oxides with a perovskite structure, the interfacial atoms are not arranged in long-distance order or short-distance order because of the variety of components. Figure 1 shows a transmission electron micrograph with high resolution which can be compared with the models given in Fig. 2. In Fig. 2 model patterns of the transverse sections of a simple nanocrystalline metal [6], a composite oxide with conventional crystals and nanocrystals are shown. It can be seen from Fig. 2 that, in the lattice, the atomic arrangement of the nanocrystalline composite oxide is generally similar to that of the nanocrystalline metal. However, because of the variety of components and the random orientation of the crystalline grains in the former, the crystalline planes appear varied and in a highly disordered state. In particular, the atoms of the various components on the crystalline surface differ from those in the lattice. Because in the nanocrystalline composite oxide, the atoms on the crystalline surface are in the "naked state", their coordinate status is unsaturated and differs from that of the same kind of atom in the bulk phase, so that they can form broken or hanging bonds; the electrons in the bonds are in the unpaired state. Because the nanocrystalline composite oxide contains a large interfacial area, there is a variety of unsaturated and broken bonds on the intercrystalline plane. Many properties of nanocrystalline composite oxides depend on the characteristics of the broken bonds. Therefore we examined the unpaired electrons in the nanocrystalline composite oxides by EPR spectroscopy and compared them with those in the conventional materials.

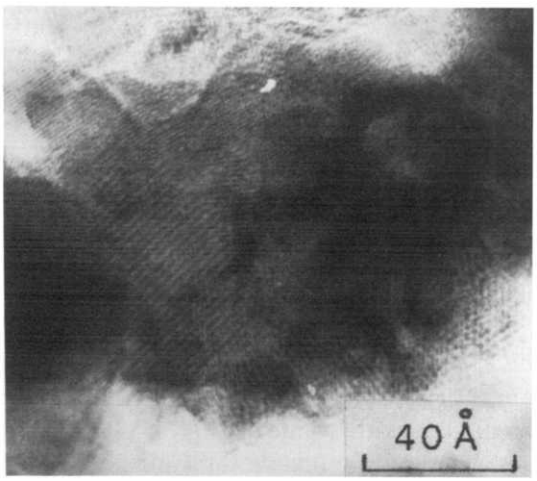

Fig. 1. Transmission electron micrograph with high resolution of sample A at a static pressure of 1.0 GPa.

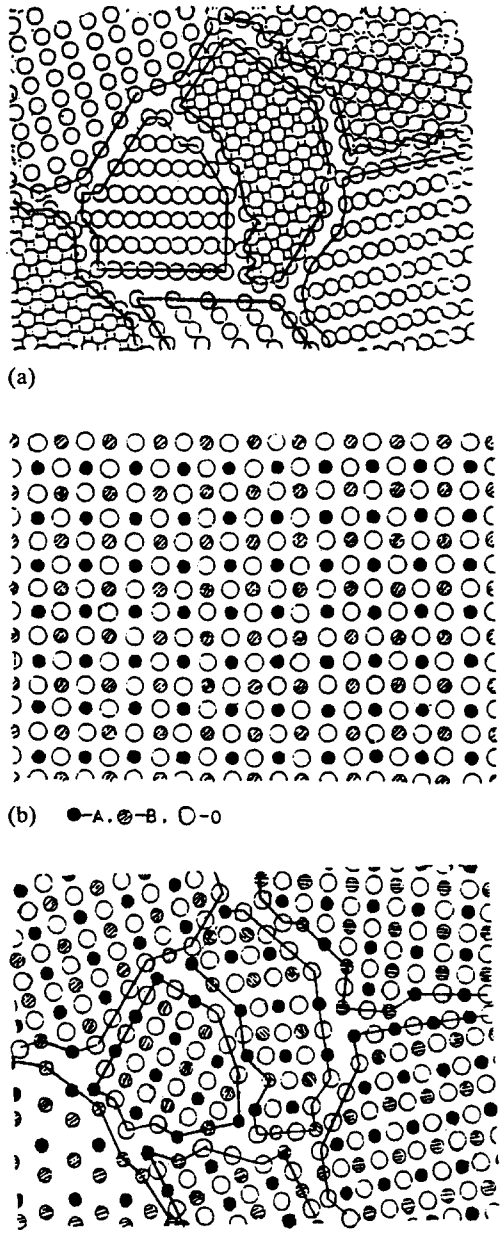

Fig. 2. Model patterns of the transverse sections of a simple nanocrystalline metal (a), composite oxide with conventional crystals (b) and nanocrystals (c).

3.2. EPR spectra of nanocrystalline composite oxides

Table 1 lists the EPR spectral parameters. Figure 3(a) shows the EPR spectra of nanocrystalline samples $La_{1-x}Sr_xFeO_3$ ($x=0.2$) obtained at different compacting pressures at ambient temperature. Figure 3(b) shows the EPR spectra of powder samples of $La_{1-x}Sr_xFeO_3$ ($x=0.1$, 0.2 and 0.4) with conventional crystals. It can be seen from Table 1 and Fig. 3 that the relative

TABLE 1. EPR spectral data of $La_{1-x}Sr_xFeO_3$ samples at ambient temperature and under different compacting pressures

Sample	d	x	Compacting pressure (GPa)	RI mg^{-1}	ΔH_{pp}	S'/S''	g value
A	12.4	0.0	0.0	69.00	120.5	1.0	2.22
			0.5	53.00	114.3	1.0	2.32
			1.0	59.00	117.4	0.88	2.33
			1.5	48.00	124.8	1.0	2.44
B	6	0.1	0.0	72.70	113.0	1.0	2.23
			0.5	77.00	110.0	1.0	2.19
			1.0	62.00	111.2	1.0	2.25
			1.5	61.60	116.0	0.86	2.23
C	4	0.2	0.0	83.00	111.0	1.0	2.19
			0.5	79.00	106.3	1.0	2.18
			1.0	89.00	106.3	1.0	2.36
			1.5	77.00	106.3	1.0	2.30
D	7	0.4	0.0	64.00	111.2	1.0	2.20
			1.0	76.00	103.8	1.0	2.26
E	8	0.6	0.0	70.00	139.1	1.0	2.40
			1.0	99.00	148.3	1.0	2.44
			1.5	74.00	142.1	1.0	2.36
F	82	0.1	0.0	0.0235	117.2	1.09	2.27
G	60	0.2	0.0	0.0323	105.0	1.0	2.31
H	70	0.4	0.0	0.101	136.0	1.0	2.18

ΔH_{pp}, the peak–peak width of spectrum lines (mT); RI mg^{-1}, relative intensity of EPR spectra per milligram $La_{1-x}Sr_xFeO_3$ sample; S'/S'', ratio of upper to lower peak area; d, mean diameter of crystalline grains (nm).

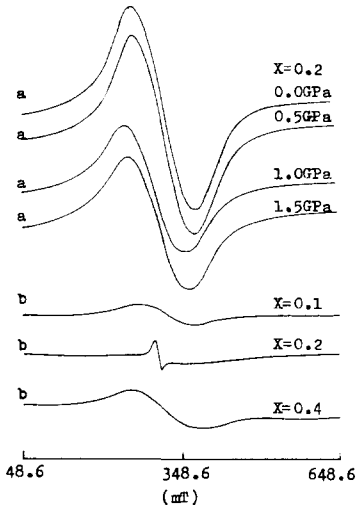

Fig. 3. (a) EPR spectra of nanocrystals $La_{1-x}Sr_xFeO_3$ ($x=0.2$) under different static pressures at ambient temperature. (b) EPR spectra of conventional crystals $La_{1-x}Sr_xFeO_3$ ($x=0.1$, 0.2 and 0.4) at ambient temperature.

intensities of the EPR spectra per milligram of sample (RI mg^{-1}) of nanocrystalline materials are about 10^3–10^4 times stronger than those of the conventional materials, and change with grain size and compacting pressure. The range of g values is typical of the trivalent iron atom, Fe(III).

3.3. The change in g value

Fe atoms in the nanocrystalline composite oxides may be divided into two kinds: on the intercrystalline plane or in the bulk phase. An Fe atom in the bulk phase coordinates with six oxygen atoms and has an unpaired electron on the 3d orbital. Because of its saturated coordination, the ABO_3 molecules are complete. The crystal fields are strong and the interaction between magnetic nuclei is also strong. The excited state is very different from the ground state in energy, and the EPR spectra of Fe atoms lying in this state are not easily observed.

Fe atoms on the crystalline surface can form unsaturated coordination with three or more oxygen atoms. Because of the existence of broken bonds, the Fe atoms form incomplete molecules with a high-spin state [10]. Because of the reduction of the coordination number, the interactions between crystal fields and the magnetic correlation are decreased giving weak-field coordination. In addition, the interaction between the magnetic nuclei and the symmetry of the lattice decreases, the spin–orbit coupling increases and the excited state is close to the ground state. Thus the paramagnetic signal increases and the g value deviates from the standard value of two.

3.4. The change in RI mg^{-1} value

Because of the large number of broken bonds on the surface of nanocrystals, the chemical bonds and electronic spin state of nanocrystals are different from those of ideal crystals. Whether nanocrystalline or conventional, defects associated with unsaturated coordination are reflected in the relative intensity of the EPR signals. The defects in the bulk phase are far less than those on the surface for nanocrystalline materials, whereas this is not true of conventional materials. It can be seen from Table 1 that the RI mg^{-1} values of the EPR signals for samples A, B, C, D and E are far larger than those for samples F, G and H, *i.e.* 10^3–10^4 times stronger. Because the size of the crystalline grains of sample C is smaller (4 nm) than those of sample D or E, the RI mg^{-1} value of this sample is larger. Similarly, although sample A does not contain Sr(II), the RI mg^{-1} value of the EPR signal is large because the grain size of the sample is small, in other words it reflects the nanocrystalline feature. In short, we consider that the changes in the EPR signals result from the defects on the surface only when the crystalline grain size is small (nanometre).

3.5. The effect of compacting pressure

The structural models shown in Figs. 2(b) and 2(c) indicate that the configuration and electronic distribution of the nanocrystalline composite oxide are very different from those of the conventional composite oxide. Because the interaction between Fe atoms decreases on the intercrystalline surface, the interaction of Fe atoms between adjacent crystalline grains increases with an increase in compacting pressure. The acting force is between van der Waals' and covalent bonds. On compacting the nanocrystalline powders into a nanocrystalline solid material under different pressures, dislocation and break up of the lattice may occur [11]. Since the partial interface of the compacted nanocrystals may be transformed into contact zones, the surface area of the crystals may decrease. When the compacting pressure is increased further, the partial crystals may suffer new dislocation and break up under the stress of the contact zones of the interparticles, and the surface area may increase. The smaller the crystal size, the lower the compacting pressure required for break up. The dislocation of the lattices, the break up of the crystals and the change in the contact zones produce the changes in the defects on the surface; therefore the RI mg^{-1} values of the EPR signals change with compacting pressure. The trend is in accord with that of Mössbauer spectra or X-ray photoelectron spectra with compacting pressure [12, 13].

Acknowledgment

This project was supported by the National Natural Science Foundation of China.

References

1 X. Zhu, R. Birringer, U. Herr and H. Gleiter, *Phys. Rev. B, 35* (1987) 9085.
2 T. Haubold and R. Birringer, *J. Less-Common Met., 145* (1988) 557.
3 R. W. Siegel and J. A. Eastman, *Mater. Res. Soc. Symp. Proc., 132* (1989) 3.
4 A. Chatterjee and D. Chakravorty, *J. Phys. D, 22* (1989) 1386.
5 C. J. Adkms, *J. Phys. C, 15* (1982) 7143.
6 R. Birringer, *Mater. Sci. Eng. A, 117* (1989) 33.
7 J. A. Cowen, B. Stolzman, R. S. Averback and H. Hahn, *J. Appl. Phys. 61* (8) (1987) 3317.
8 X. Li, B. Xu, Z. Wang, F. Chi and M. Zhao, *J. Mater. Sci. Lett.*, in press.
9 X. Li, B. Xu. Z. Wang, F. Chi and M. Zhao, *J. Chin. Chem. Lett., 3* (1) (1992) 77.
10 X. Li, F. Chi, B. Xu, M. Zhao and Y. Zheng, *J. Phys. D,* in press.
11 E. Tronc, J. P. Jolivet and J. Livage, *Hyperfine Interact., 54* (1990) 737.
12 X. Li, X. Cui, X. Liu, M. Jin, L. Xiao and M. Zhao, *Chem. J. Chin. Univ. (Engl. Ed., 8* (2) (1992).
13 X. Li, X. Liu, B. Xu and M. Zhao, *J. Alloys Comp.*, in press.